© 2025. Published by The Company of Biologists | Journal of Experimental Biology (2025) 228, jeb250373. doi:10.1242/jeb.250373

RESEARCH ARTICLE

When size matters: energy allocation and thermogenic mechanisms in very small mammals, African pygmy mice

Mélanie Boël[1,2,*], Léa Herpe[3,4], Claude Duchamp[4], Caroline Romestaing[4], François-Xavier Dechaume-Moncharmont[4], Loïc Teulier[4], Frédéric Veyrunes[5], Damien Roussel[4], Nicolas Pichaud[3] and Yann Voituron[4]

ABSTRACT

Thermoregulation is a major challenge for extremely small mammals such as the African pygmy mice *Mus mattheyi* and *Mus minutoides*, weighing less than 12 g. A previous study showed that these tiny mice exhibit different mitochondrial energy efficiency for ATP synthesis, with a higher efficiency in *M. mattheyi* (~6 g) than in *M. minutoides* (~10 g). This result suggests a lower mitochondrial heat production at rest in *M. mattheyi*, despite its lower body surface and inevitably greater heat loss from its body surface, than in *M. minutoides*. Consequently, a compensatory thermoregulatory strategy should exist in *M. mattheyi* to maintain homeothermy. The present study aimed to assess whether *M. mattheyi* uses non-shivering thermogenesis in brown adipose tissue (BAT) and/or activity-thermoregulatory heat substitution. For this purpose, multidisciplinary approaches involving behavioral, physiological, biochemical and molecular analyses were used. *Mus mattheyi* showed higher daily mass-specific energy expenditure and food intake per unit mass and allocated more daily energy to vital function, spent less time moving in their cage during the daytime but exhibited higher non-locomotor activity and higher movement-related energy cost compared with *M. minutoides*. BAT of *M. mattheyi* was metabolically more active, exhibiting higher mitochondrial respiration rates and citrate synthase activity than in *M. minutoides*, but lower uncoupling protein 1 content. Altogether, these results suggest that the tiny *M. mattheyi* mainly uses non-exercise activity thermogenesis, increased cost of movement and, to a lesser extent, BAT non-shivering thermogenesis for remaining warm.

KEY WORDS: *Mus mattheyi*, *Mus minutoides*, Oxidative phosphorylation, Brown adipose tissue, Skeletal muscle

INTRODUCTION

In mammals and birds, endothermy ensures a high degree of thermal independence from ambient temperature, enabling endotherms to maintain optimal enzyme function, muscle performance and neurological processes across a wide range of environmental temperatures (Hillenius and Ruben, 2004). However, endothermy imposes high energetic demands to fuel the metabolic rates required to regulate core body temperature at a set point independent of ambient temperature (McNab, 2002). This thermoregulation process is intricately linked to metabolic processes and represents a major energy challenge for mammals, especially for small species that exhibit a high surface-to-volume ratio, and consequently a high heat dissipation through the body surface (Reynolds, 1997). To compensate for high heat dissipation, small mammals increase their mass-specific metabolic rate more compared with larger species. The metabolic rate is fundamentally connected to mitochondrial functioning, which is primarily involved in ATP synthesis, the primary energy currency of cellular activity. Consequently, mitochondria in small species consume more oxygen and nutrients, synthesizing ATP with a higher energy cost and lower coupling efficiency compared with larger organisms (Gavrilov et al., 2022; Glazier, 2005; Hatton et al., 2019).

Within cells, the conversion of oxygen and nutrients into ATP molecules through oxidative phosphorylation (OXPHOS) is inherently imperfect, inevitably leading to heat dissipation that can be used as a thermogenic mechanism (Brand et al., 1991; Bertholet and Kirichok, 2021). Proton leakage across the mitochondrial inner membrane bypasses ATP production, dissipating the proton gradient as heat (Divakaruni and Brand, 2011; Jastroch et al., 2010; Rolfe and Brown, 1997). Mitochondria are considered as a potential necessary heat generating source within organisms (El-Gammal et al., 2022; Macherel et al., 2021). Interestingly, mitochondrial efficiency positively correlates with body mass in endotherms, with small endotherm species exhibiting less efficient skeletal muscle and liver mitochondria at rest, i.e. consuming more oxygen and nutrients to produce the same amount of ATP, and therefore generating more heat as a by-product (Mélanie et al. 2019; Boël et al., 2023; Barbe et al., 2023). *Mus minutoides* was the species with the least efficient mitochondria compared with the other species (Mélanie et al. 2019; Boël et al., 2023). In this general framework, the pygmy mouse *Mus mattheyi* arises as an exception. Indeed, this very small mouse (4–8 g) has mitochondria that use oxygen and nutrients more efficiently for ATP production than expected for its small body mass, particularly when compared with the closely related *M. minutoides* (7–14 g) (Boël et al., 2020). While such surprisingly high mitochondrial coupling efficiency could reduce the high energetic cost associated with its very small size, it simultaneously limits mitochondrial heat production at rest, potentially exposing this tiny endotherm to significant cooling risk.

To avoid hypothermia, several adaptations could occur: (i) behavioral huddling to keep warm within the nest (Groó et al., 2018; Mota-Rojas et al., 2021; Nowack and Geiser, 2016); (ii) entering torpor by lowering body temperature and metabolic rate (Nowack et al., 2023; Heldmaier et al., 2024; Turbill et al., 2024); or (iii) enhancing the thermogenic capacities of specific tissues, such

[1]Université Claude Bernard Lyon 1, LEHNA UMR 5023, CNRS, ENTPE, 69518 Vaulx-en-Velin, France. [2]Université de Rennes, Ecosystèmes, Biodiversité, Evolution – ECOBIO UMR 6553, CNRS, 35042 Rennes, France. [3]Université de Moncton, Département de chimie et biochimie, Moncton, NB, Canada, E1A 3E9. [4]Université Claude Bernard Lyon 1, LEHNA UMR 5023, CNRS, ENTPE, 69622 Villeurbanne, France. [5]Université de Montpellier, ISEM UMR 5554, CNRS, IRD, 34095 Montpellier, France.

*Author for correspondence (melanie.boelvoisin@entpe.fr)

M.B., 0000-0003-4286-6139

Received 13 February 2025; Accepted 16 July 2025

as brown adipose tissue (BAT) and/or skeletal muscle through diverse cellular mechanisms.

BAT is mainly responsible for non-shivering thermogenesis (Cannon and Nedergaard, 2004; Fenzl and Kiefer, 2014; Klingenspor, 2003) through the activity of mitochondrial uncoupling protein 1 (UCP1), located in the inner membrane. This protein uncouples ATP production from oxygen consumption, thereby generating heat (Bertholet and Kirichok, 2017; Cannon and Nedergaard, 2004; Fedorenko et al., 2012; Matthias et al., 2000; Nicholls, 2006). Skeletal muscle can also generate heat by non-shivering thermogenesis through sarcoplasmic reticulum calcium pumping and futile cycles (Bal and Periasamy, 2020; de Meis, 2002; Periasamy et al., 2017). At the same time, a potentially important behavioral thermoregulatory mechanism has been described in several endotherms. Known as heat substitution through locomotor activity, this mechanism involves rerouting heat from active skeletal muscles to the body's core (Brown et al., 1991; Girardier et al., 1995; Liwanag et al., 2009). As a result, physical activity can replace the heat that a resting endotherm should have produced through thermogenesis, providing 'heat for nothing or activity for free' (Humphries and Careau, 2011).

In the present study, we investigated the potential behavioral and physiological thermogenic mechanisms of two closely related species exhibiting contrasting mitochondrial functioning: *M. mattheyi* and *M. minutoides*. We hypothesized that *M. mattheyi* uses the surplus of ATP produced by these more efficient muscle mitochondria to exhibit greater locomotor activity, enabling it to take advantage of the heat released by its skeletal muscles. If increased locomotion is not demonstrated, we hypothesized a higher BAT activity in *M. mattheyi* enabling it to produce heat through non-shivering thermogenic mechanisms. To assess these hypotheses, the energy expenditure, caloric and water intake, as well as non-locomotor, locomotor and resting behaviors were measured. We also measured the number of crossings made by individuals in cages, the energy cost of a movement and the mitochondrial respiration in skeletal muscle and BAT. Finally, we investigated the activity of three enzymes involved in different metabolic pathways [citrate synthase (CS), β-hydroxyacyl-coenzyme A dehydrogenase (HOAD) and carnitine palmitoyltransferase (CPT)] as well as the abundance of different mitochondrial proteins [UCP1, ATP synthase F1 subunit beta (ATP5b), mitochondrial import receptor subunit (TOM20) and superoxide dismutase 2 (SOD2)] in BAT.

MATERIALS AND METHODS

All experiments were conducted in accordance with animal care guidelines and were approved by the ethics committees of Lyon (France), as well as the Ministry of Research and Higher Education (Ministère de la Recherche et de l'Enseignement Supérieur) (APAFIS#27770-2020102212072365).

Animal care and housing

Adult males of two closely related African pygmy mouse species (Britton-Davidian et al., 2012; Veyrunes et al., 2005) were used: *Mus mattheyi* Petter 1969 (n=13) and *Mus minutoides* (A. Smith 1834) (n=13). All individuals were supplied by a breeding and experimentation center for animal models (Centre d'Élevage et de Conditionnement Expérimental des Modèles Animaux, University of Montpellier, France). They were individually housed in an experimental animal facility (Animalerie Conventionnelle et Sauvage d'Expérimentation de la Doua, University of Lyon 1, France), in house mouse cages (331 mm×159 mm×132 mm) containing sawdust, cotton, shelter and cardboard cylinders, with food and water provided *ad libitum*. Previous studies showed that the thermal neutral zone for these species is between 32 and 34°C (Downs and Perrin, 1996; Hoole et al., 2019). For this reason, the environmental temperature was maintained at 29.1±0.2°C (measured by thermometer) in the experimental room in order to approach their thermal neutral zone in experimental cages. The ambient temperature used in the study was close but still below the thermoneutral zone of these mice, which forced mice to thermoregulate to compensate for increased heat loss at the body surface. A photoperiodic cycle of 12 h:12 h night:day was established. Before any measurements, the mice underwent a 5 day acclimation phase to avoid stress caused by the change of holding conditions. African pygmy mice were fed *ad libitum* with a mixture of seeds (white millet, oatmeal, red millet, canary grass, flax and hempseed) agglomerated in the form of cookies using egg white. All individuals were weighed every 2 days for the entire experimental period to access their health condition, except during the experimental procedure (see 'Locomotor and non-locomotor behavioral analysis' and 'Energy expenditure', below). At the time of experiments, the mean±s.d. body mass was 6.1±0.9 g for *M. mattheyi* and 9.9±2.2 g for *M. minutoides* (Fig. S1). Two *M. mattheyi* reached critical ethical points, by losing between 13% and 15% of their body mass, and were removed from the procedure according to the animal care guidelines. One *M. minutoides* was also removed after being found injured in the experimental system.

Locomotor and non-locomotor behavioral analysis

Two days before behavioral measurements, all 11 *M. mattheyi* and 11 of the 12 *M. minutoides* were randomly selected to achieve a balanced sampling design. They underwent a habituation period to their new metabolic cage by slightly reducing the enrichment of their cage. The cardboard shelter was changed for a plastic one with a wall that appeared opaque black under daylight conditions but fully transparent under infrared illumination. This allowed for observations of behavior during the night when the mice are the most active. All mice were fed and watered *ad libitum* during behavior recordings and metabolic measurements. Metabolic cages enabled simultaneous recording of behavior and energy expenditure.

Behavior was monitoring with cameras (ABUS Analogue HD Video Surveillance 8-Channel Hybrid complete set) that were placed facing the longest side of the metabolic cages, with one camera for two cages. Recording of individual behavior lasted for 24 h after the habituation period. The behavior was analyzed for each individual for 5 min every quarter of an hour, for a total of 8 h over 24 h (4 h during the day and 4 h at night). Non-locomotor activity was assessed by the time spent (min) grooming, jumping, turning around, interacting with cage accessories, eating, drinking and standing up on their hindlegs; therefore, it did not include walking and running. Locomotor activity of the mice was assessed by the time spent running or walking. Rest was estimated by the time spent remaining motionless inside or outside the shelter. As infrared cameras were not operating under daylight conditions, the behavior in the shelter could not be observed during the day. Hence, the individuals hidden in their nest during the day were therefore considered to be at rest.

Energy expenditure

Simultaneously to behavior recording, oxygen consumption and carbon dioxide production of the mice were recorded by indirect calorimetry, in an open circuit with the TSE PhenoMaster (TSE

Journal of Experimental Biology (2025) 228, jeb250373. doi:10.1242/jeb.250373

Systems, Bad Homburg, Germany) equipped for multiple measurements of four individual mouse metabolic cages and an empty reference cage. Mass flow controllers (accuracy 1.1%) were used to control the inlet air flow of metabolic chambers (0.35 l min^{-1}) and gas analyzers (0.25 l min^{-1}). Residual air volume of metabolic cages was reduced to around 2 l with solid materials to comply with the small size of the animals. This reduced air volume in the metabolic cages enabled 99% equilibrium of the air in the cage to be reached within ∼26 min with the air flow rate used (Lasiewski et al., 1966) without affecting too much the activity of the animal. Air samples from each metabolic cage were analyzed every 10 min, and for 2 min to ensure sufficient stabilization, with a high-speed Siemens Ultramat/Oxymat 6 O_2/CO_2 analyzer in a measuring range between 20.26% and 20.95% for O_2 and 0.04% and 1.05% for CO_2. The analyzer was calibrated at the beginning and at the end of each measurement session with air and a gas mixture containing 20.24% O_2 and 0.94% CO_2 (Air Liquide, Paris, France). Metabolic rate was monitored for 3 days but only the last 24 h of the experiment were evaluated to avoid potential initial bias of habituation to the metabolic cages. Rates of oxygen consumption and carbon dioxide production were calculated by the TSE LabMaster system, considering the measurement of oxygen and carbon dioxide inflow from the reference cage. Metabolic rate (MR) was calculated from oxygen consumption rate ($\dot{V}_{O_2}$) and carbon dioxide production rate ($\dot{V}_{CO_2}$) according to the manufacturer's guidelines (PhenoMaster Software, TSE Systems) for mice with the formula $MR=3.941+1.106\times RER\times\dot{V}_{O_2}\times0.001$ [in kcal h^{-1} kg^{-1}, where the respiratory exchange ratio (RER) was calculated from the ratio between CO_2 production and O_2 consumption, $\dot{V}_{CO_2}/\dot{V}_{O_2}$] and then converted to mW g^{-1}.

As African pygmy mice are nocturnal species, the minimal energy expenditure (EE_{min}) was estimated by the mean of the 15% lower values obtained during the daytime (rest period) and the maximal energy expenditure (EE_{max}) by the mean of the 15% higher values recorded during the night-time (activity period), for the last 24 h. Individuals were weighed before and after the experimental procedure to observe changes in mass over time. A significant interaction between species and time of day was revealed (P=0.011) and inter-individual variance was significant in the model (χ^2_1=81.046, P<0.001). *Mus minutoides* was heavier than *M. mattheyi* both at the beginning and at the end of the experiment (P<001; Fig. S1). *Mus mattheyi* did not lose body mass during the experimental procedure (P=0.96), whereas *M. minutoides* lost about 3% of its initial body mass (P=0.002; Fig. S1). *Mus minutoides* was reared for a shorter period than *M. mattheyi*, and therefore showed more wild or less calm behavior than *M. mattheyi*. The experimental procedure may have induced a slightly greater stress in *M. minutoides*, leading to a small though statistically significant loss of body mass that remained much lower than the mass loss acceptable for conclusive experimental procedure (Silverman et al., 2014).

To consider the body mass effect between the two species, EE_{min} and EE_{max} were expressed in mW g^{-1}. In addition, the area under the actually measured EE curve (Fig. 1) represents the energy expenditure over 24 h (expressed in arbitrary units presented in the text and figures). From the energy expenditure of individuals over 24 h, the proportion of energy expenditure allocated to (i) basal functions such as maintenance, thermoregulation, digestion or endocrine regulation [area below EE_{min} or area under the curve (AUC) basal functions] and (ii) other functions such as locomotion (area above EE_{min} or AUC other functions) were estimated (Fig. 1).

Food and water intake

Food and water intake were also monitored by the TSE PhenoMaster system for the 3 days of the experiment. The residual food found in their cage at the end of the experiment was weighed and subtracted from this amount to give the mass of food ingested during these 3 days. In the same way, as the water was given in cups, the evaporation of the water for 3 days was estimated using cups placed in the reference cage (without individuals). The results of food and water intake were expressed in g day^{-1} g^{-1} body mass. In addition, the frequency of food intake was estimated by counting the number of times individuals went out to eat for the duration of the video recording studied (4 h at night and 4 h during the day), thanks to a behavioral analysis, to complete the energy expenditure and food intake data presented above.

Energy cost of movement

For this section, data were taken from the previous experimental procedures, in which mice were placed in metabolic cages to assess their behavior and energy expenditure. On the videos, the cage was divided into four virtual quadrants of equal dimension, by defining one horizontal and one vertical line on the front side of the cage, in order to score the number of transitions between either the horizontal line (movements between right and left sides of the cage), or the vertical line (when the individual climbed into the feeder).

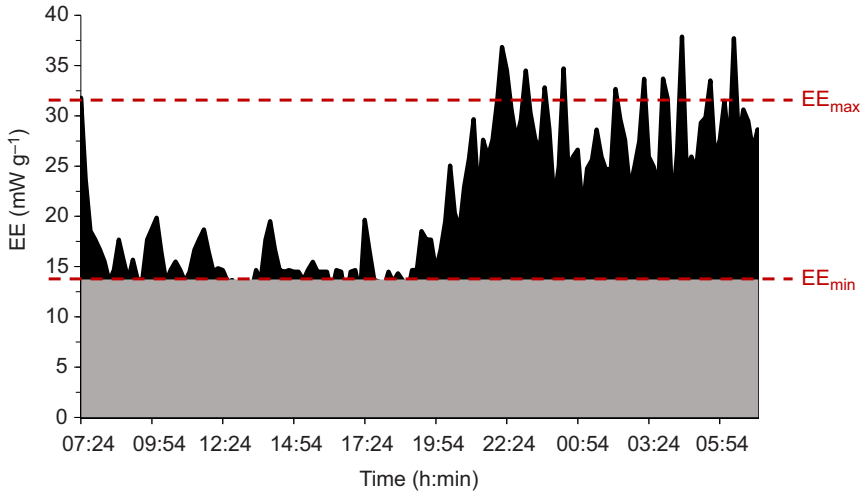

Fig. 1. Energy expenditure of one of the mice over 24 h. Energy expenditure (EE) was determined by indirect calorimetry at an ambient temperature of 29°C. EE_{min} is the mean of the 15% lowest values of EE obtained during the daytime (resting period) and EE_{max} is the mean of the 15% highest values of EE recorded during the night-time (period of activity). The gray area corresponds to the energy allocated to basal functions (e.g. respiration, thermoregulation, digestion) of the organism and the black area represents the energy used for other biological functions (locomotion, for example). The proportion of energy allocated to basal or other biological functions was calculated according to the following formula: (gray or black area/total area)×100.

The energy cost of a movement expressed in mW g^{-1} $crossing^{-1}$ was calculated for the day and night periods, using the following formula: AUC for other functions (such as locomotion)/no. of crossings during the period studied. The AUC for the other functions was determined as described above (see 'Energy expenditure').

Respiratory capacity of BAT and skeletal muscle

The African pygmy mice used for behavioral and metabolic measurements, as well as the *M. minutoides* mouse kept in reserve, were weighed and killed by cervical dislocation (11 *M. mattheyi* and 12 *M. minutoides*). Then, the gastrocnemius muscle and the intrascapular BAT samples were mechanically dissected with scissors from the mice. The intrascapular BAT was weighed to estimate its proportion for each individual (g BAT g^{-1} animal). BAT was then separated: one part was directly placed in cold isolation buffer (BIOPS: 2.77 mmol l^{-1} Ca-K_2EGTA, 7.23 mmol l^{-1} K_2EGTA, 20 mmol l^{-1} imidazole, 20 mmol l^{-1} taurine, 50 mmol l^{-1} K-MES, 0.5 mmol l^{-1} dithiothreitol, 6.5 mmol l^{-1} $MgCl_2$, 5.77 mmol l^{-1} Na_2-ATP, 15 mmol l^{-1} phosphocreatine; pH 7.2), and gently torn apart with fine forceps to achieve mechanical permeabilization to measure mitochondrial oxygen consumption; the other part was snap frozen for further biochemical analysis (see 'Enzymatic activity and relative abundance of proteins in BAT'). Gastrocnemius muscle was then dissected transversally in BIOPS in order to get a mix of red (rather oxidative and inner) and white (rather glycolytic and outer) fibers. Muscle fibers were firstly separated mechanically with forceps and then chemically with saponin (50 µg ml^{-1}) according to a standard protocol (Pesta and Gnaiger, 2012). Permeabilized fibers and interscapular BAT were weighed and placed in a high-resolution respirometer glass-chamber (Oxygraph-2K, Oroboros Instruments, Innsbruck, Austria) containing hyper-oxygenated respiratory buffer heated at 37°C (MiR05: 110 mmol l^{-1} sucrose, 0.5 mmol l^{-1} EGTA, 3 mmol l^{-1} $MgCl_2$, 60 mmol l^{-1} potassium lactobionate, 20 mmol l^{-1} taurine, 10 mmol l^{-1} KH_2PO_4, 20 mmol l^{-1} Hepes and 1 g l^{-1} fatty acid-free bovine serum albumin; pH 7.1). Respiration measurements were performed between 400 and 200 µmol l^{-1} oxygen.

To obtain leak respiration of the tissue, at the level of complex I (CI-LEAK), a mixture of pyruvate (5 mmol l^{-1}) and malate (2.5 mmol l^{-1}) was added. The phosphorylating respiration (CI-OXPHOS) was obtained after addition of ADP (1 mmol l^{-1}). The integrity of the permeabilized fibers was checked by measuring oxygen consumption in the presence of cytochrome *c* (10 µmol l^{-1}). Subsequently, succinate (5 mmol l^{-1}) was injected to stimulate complex II of the electron transfer system (CI+CII-OXPHOS) and glycerol 3-phosphate (10 mmol l^{-1}), which provides electrons to the electron transfer system via mitochondrial glycerol 3-phosphate dehydrogenase (CI+CII+G3PDH-OXPHOS) (McDonald et al., 2018; Mráček et al., 2013). The fully uncoupled respiration (MaxETS) representing the maximal capacity of the electron transfer system was obtained with the addition of carbonyl cyanide *p*-tri-fluoromethoxy-phenylhydrazone (FCCP, 2 µmol l^{-1}). Residual oxygen consumption obtained after addition of antimycin (2.5 µmol l^{-1}), inhibiting respiration due to substrates, was subtracted from other respiratory states. Then, the maximal capacity of the cytochrome *c* oxidase (COX) by the addition of ascorbate (2.5 mmol l^{-1}) and of *N*,*N*,*N*′*N*′-tetramethyl-1,4-phenylenediamine (TMPD, 0.5 mmol l^{-1}) was determined. The COX maximal capacity was corrected for ascorbate/TMPD auto-oxidation after inhibition of complex IV by potassium cyanide (1 mmol l^{-1}).

Variation in the mass-specific oxygen consumption rates obtained (pmol O_2 s^{-1} mg^{-1} tissue) is indicative of both qualitative (function) and quantitative (mitochondrial number/density) changes. Thus, these rates were divided by COX maximal capacity as an internal normalizer to properly compare the two species and reveal the possible different proportions of each complex for each species (Picard et al., 2011; Pichaud et al., 2011).

Enzymatic activity and relative abundance of proteins in BAT

Samples of BAT, collected as detailed above (see 'Respiratory capacity of BAT and skeletal muscle') from 11 *M. mattheyi* and 12 *M. minutoides* for mitochondrial respiration measurements were used. Frozen BAT was weighed and separated in two. The first part was homogenized in phosphate-buffered saline (PBS: 137 mmol l^{-1} NaCl, 2.7 mmol l^{-1} KCl, 10 mmol l^{-1} Na_2HPO_4, 1.8 mM KH_2PO_4, pH 7.4) for the measurement of enzymatic activity and the second part was homogenized in radioimmunoprecipitation assay (RIPA) buffer (Sigma-Aldrich) supplemented with 1% protease inhibitor cocktail and 2 mmol l^{-1} sodium orthovanadate for the quantification of protein abundance.

Enzymatic activity

The homogenates were centrifuged at 1000 ***g*** for 10 min at 4°C and the supernatant was collected for measurement of enzymatic activity, using a BioTek Synergy H1 microplate reader (Biotek, Montréal, QC, Canada) set at 37°C. All protocols were adapted from Bergmeyer (1983), and enzymatic activity is expressed as U mg^{-1} of tissue, where U represents 1 µmol of substrate transformed to product in 1 min.

CS is the first mitochondrial enzyme involved in the tricarboxylic cycle that feeds the mitochondrial respiratory chain with reduced coenzymes (Chhimpa et al., 2023). CS (EC 4.1.3.7) activity in tissue was measured at 412 nm for 8 min by following the reduction of 5,5′-dithiobis-2-nitrobenzoic acid (DTNB, ε=13.6 ml cm^{-1} $µmol^{-1}$) using a 100 mmol l^{-1} imidazole-HCl buffer containing 0.1 mmol l^{-1} DTNB, 0.1 mmol l^{-1} acetyl CoA and 0.15 mmol l^{-1} oxaloacetic acid (omitted from the blank), pH 8.0.

β-hydroxyacyl-coenzyme A dehydrogenase (HOAD) is involved in β-oxidation and frequently used as a quantitative index for lipid catabolism (Jayasundara et al., 2015). HOAD (EC 1.1.1.35) activity was evaluated in a 100 mmol l^{-1} triethanolamine-HCl buffer complemented with 5 mmol l^{-1} EDTA, 1 mmol l^{-1} KCN, 0.115 mmol l^{-1} NADH and 0.05 mmol l^{-1} acetoacyl CoA (omitted from the blank), pH 7.0, by recording the disappearance of NADH at 340 nm (ε= 6.22 ml cm^{-1} $µmol^{-1}$) for 8 min.

CPT facilitates the transfer of long-chain fatty acids from the cytoplasm into the mitochondria during the oxidation of fatty acids (Joshi and Zierz, 2020). CPT (CPT, EC 2.3.1.21) activity was measured for 8 min by following the reduction of DTNB (ε=13.6 ml cm^{-1} $µmol^{-1}$) in the presence of a Tris-HCl buffer (75 mmol l^{-1} Trizma base, 5 mmol l^{-1} EDTA, pH 7.0) complemented with 2 mmol l^{-1} L-carnitine and 0.035 mmol l^{-1} palmitoyl-coenzyme A (omitted from the blank).

Abundance of proteins

Protein homogenates were first centrifuged at 6000 ***g*** for 15 min at 4°C and the supernatant was collected without the fat layer, and centrifuged again at 12,500 ***g*** for 10 min at 4°C. The resulting supernatant was used to measure protein concentration determined by the Bradford assay (Hammond and Kruger, 1988). Proteins were loaded in each well and resolved in 4–15% SDS-PAGE Mini-PROTEAN TGX Stain-Free Gels (Bio-Rad, Hercules, CA, USA), transferred to PVDF membranes (Bio-Rad), and blocked for 1 h with 5% skimmed milk. Membranes were probed overnight at 4°C with primary antibodies against UCP1 (Cell signaling; 14670S), TOM20

Journal of Experimental Biology (2025) 228, jeb250373. doi:10.1242/jeb.250373

(Santa Cruz; sc-17764), ATP5b (Abcam; ab14730) and SOD2 (Cell signaling; 13194S) (1:1000 dilution for all). These proteins were chosen to represent different mitochondrial compartments and to evaluate mitochondrial thermogenesis with UCP1. TOM20 is a protein found in the outer mitochondrial membrane which functions as a component of the import receptor complex for mitochondrial precursor proteins synthesized in cytoplasm (Schleiff and Turnbull, 1998). ATP5b codes for the β-subunit of F0-F1 ATP synthase, which is located in the inner mitochondrial membrane and involved in the synthesis of ATP (Habersetzer et al., 2013; Xu et al., 2021). SOD2 is located in the mitochondrial matrix and is considered to be one of the antioxidant systems with the highest potential for neutralization of ROS (Palma et al., 2020). Protein bands were revealed by probing for 1 h with HRP-conjugated anti-mouse or anti-rabbit antibodies (1:5000 dilution). Immunoblots were visualized by chemiluminescence and images were taken with a Chemidoc Touch Imaging System (Bio-Rad), and the densitometric analyses were performed using Image Lab v.6.1.0 software (Bio-Rad) with abundance normalized using the stain-free method. All samples from *M. minutoides* were used, while for *M. mattheyi* it was only possible to carry out measurements on eight individuals as the quantity of biological sample was insufficient for the three other individuals.

Statistical analysis

All statistical analyses were performed with R software 4.3.1 (http://www.R-project.org/). Linear mixed-effect models (Bates et al., 2015), with individual identity as a random variable, were used to evaluate the effects of (i) species and period of the day on body mass transformed by a cube root function, (ii) species and behavioral category (non-locomotor activity, locomotor activity or rest) on the time spent in performing a behavior transformed by a cube root function, (iii) species and type of function (vital or other functions) on the energy allocation during the day and night, (iv) species and period of the day on the respiratory quotient, (v) species and period of the day on the number of crossings made by individuals transformed by a cube root function, (vi) species and period of the day on the energy cost of a movement transformed by a cube root function, and (vii) species and substrates on mitochondrial respiration transformed by a square root function in the BAT and the skeletal muscle. Assumption about normality and homoscedasticity of the residues for the linear mixed models were assessed by inspection of diagnostic plots. ANOVA tests (https://CRAN.R-project.org/package=car) were performed and estimated marginal means (EMMs, https://CRAN.R-project.org/package=emmeans) were calculated for *post hoc* pairwise comparisons from the linear mixed models previously described (Tables S1 and S2). Inter-individual effect in the models was statistically tested with an ANOVA comparing the linear model with or without the individual as random factor. Finally, as the dataset is small, permutation *t*-tests with a fixed number of permutations of 1000 (https://CRAN.R-project.org/package=MKinfer), based on the empirical distribution of the data, were used to assess the effect of species on (i) EE_{min} and EE_{max}, (ii) the EE of individuals over 24 h, (iii) food and water intake, (iv) BAT proportion, (v) MaxETS respiration rate in the BAT and the skeletal muscle, (vi) enzymatic activity (CS, HOAD, CPT) and (vii) protein abundance (UCP1, ATP5b, TOM20, SOD2). For all statistical analyses, a risk factor of 0.05 was used. Values in the text are presented as means±s.d.

RESULTS

Locomotor and non-locomotor behavioral analysis

An interaction between mouse species and behavior category was highlighted, irrespective of the period of the day ($P<0.001$ for daytime and $P=0.028$ for night-time). During the day, *M. mattheyi* was more active on-site ($P=0.004$), but walked/ran significantly less than *M. minutoides* ($P=0.032$; Fig. 2A). The two species spent an equivalent amount of the daytime resting ($P=0.59$): 190±17 min for *M. mattheyi* and 204±20 min for *M. minutoides* (Fig. 2A). *Mus mattheyi* spent finally 0.57% of its daytime walking/running, 20.30%

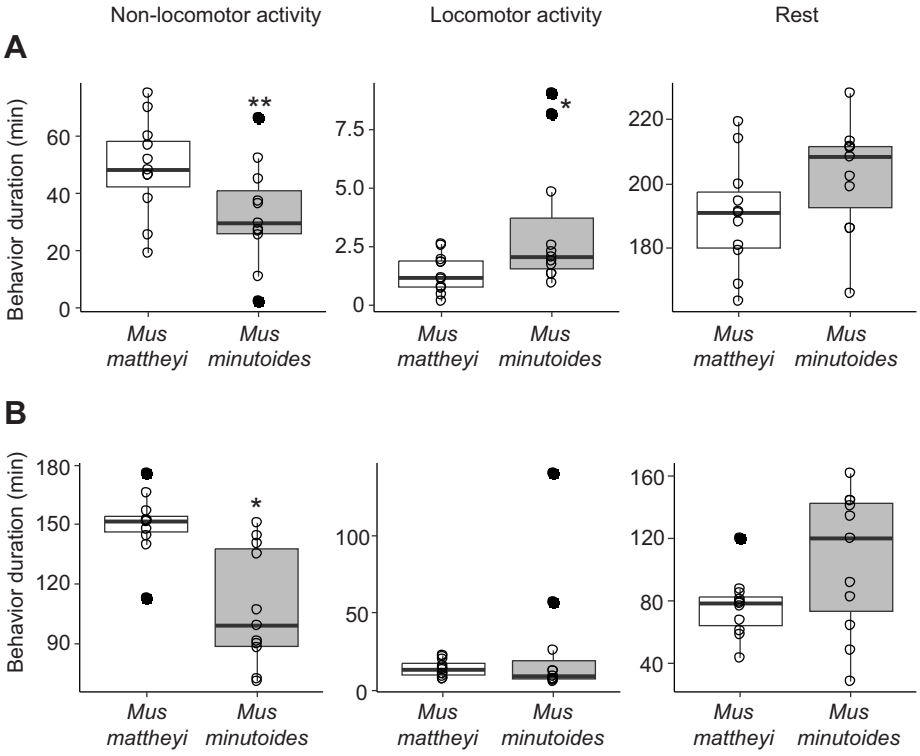

Fig. 2. Behavior analysis of African pygmy mice. The behavior of *n*=11 *Mus mattheyi* (white) and *n*=11 *Mus minutoides* (gray) was recorded during the day (A) or during the night (B). Behavior duration is presented according to three behavioral categories: non-locomotor activity, locomotor activity and rest. Behavior was analyzed for each individual for 5 min every quarter of an hour, for a total of 4 h during the day and 4 h at night. For each box plot, the horizontal line denotes the median, the box represents the interquartile range (IQR; 25th–75th percentiles), and whiskers indicate the range of values within 1.5× IQR from the lower and upper quartiles. Outliers are indicated by filled circles and were considered in statistical analyses. The results were statistically analyzed by ANOVA and estimated marginal means (EMMs) pairwise comparisons on linear mixed-effect models: **P*<0.05 and ***P*<0.01 *M. mattheyi* versus *M. minutoides*.

Journal of Experimental Biology (2025) 228, jeb250373. doi:10.1242/jeb.250373

showing non-locomotor activity and 79.13% resting. In contrast, *M. minutoides* spent 1.37% of its time in walk/run, 13.56% active on-site and 85.07% resting. As nocturnal species, they spent globally less time resting and were more active at night (Fig. 2B). *Mus mattheyi* showed more non-locomotor activity compared with *M. minutoides* (P=0.040; Fig. 1B). In addition, *M. mattheyi* spent as much time moving around and resting as *M. minutoides*: 20±29 min walk/run and 91±37 min resting for both species (P=0.45 for locomotor activity and P=0.15 for resting; Fig. 2B). *Mus mattheyi* spent thus 5.80% of its time to locomotor activity, 62.53% moving on-site and 31.67% resting. While *M. minutoides* spent 11.07% of its time walking/running, 45.01% showing non-locomotor activity and 43.92% resting.

Energy expenditure

Mass-specific EE_{min} and EE_{max} of *M. mattheyi* were higher than those of *M. minutoides* (t=5.230, P<0.001 for EE_{min}; t=5.122, P<0.001 for EE_{max}; Fig. 3A). Mass-specific EE_{min} was 16.4 ±2.5 mW g^{-1} for *M. mattheyi* and 11.3±2.0 mW g^{-1} for *M. minutoides*. During the night, energy expenditure was higher than during the day for both species: mass-specific EE_{max} was 35.6±4.7 mW g^{-1} for *M. mattheyi* and 26.6±3.5 mW g^{-1} for *M. minutoides*. Finally, energy expenditure over 24 h in *M. mattheyi* (AUC total) was 1.3-fold higher than that of *M. minutoides* (t=4.935, P<0.001): 34,764±5027 and 25,924 ±3129 arbitrary units for *M. mattheyi* and *M. minutoides*, respectively.

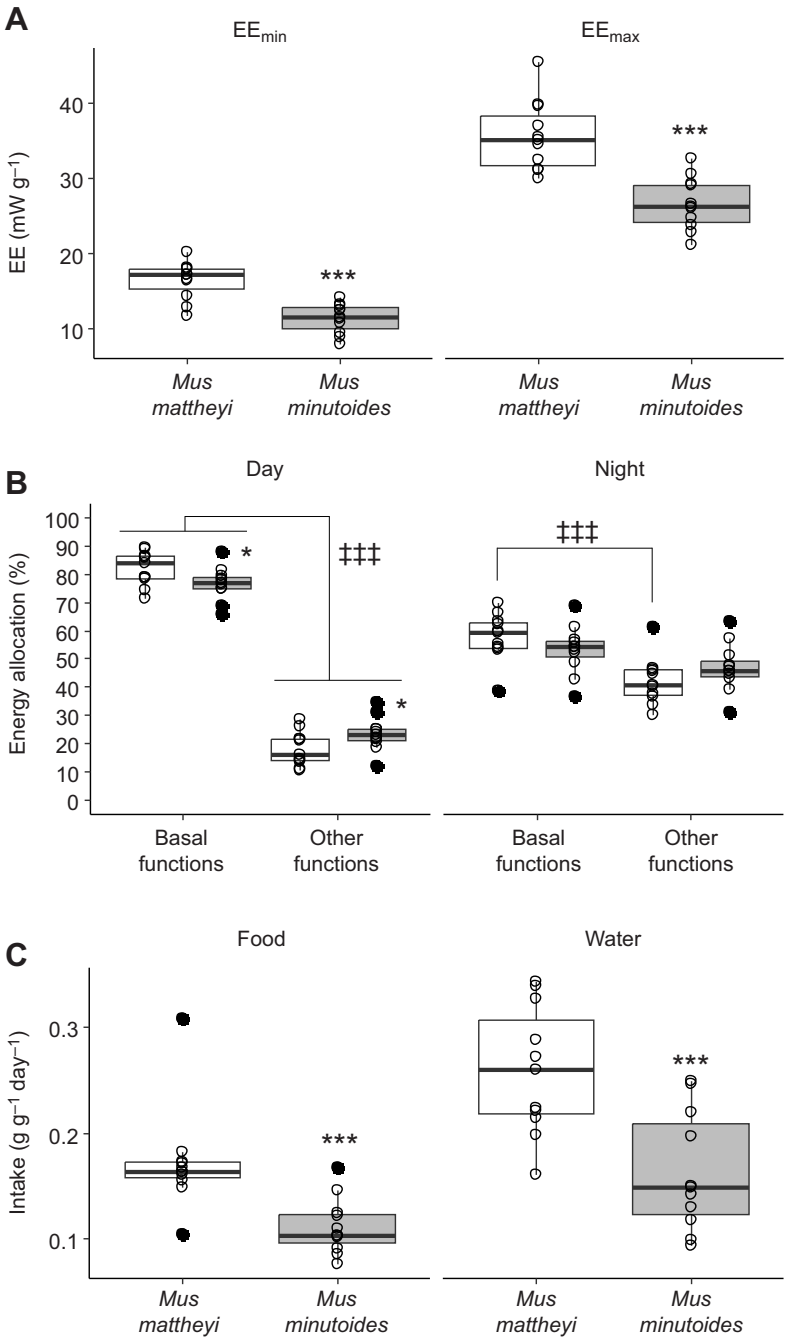

Fig. 3. Energy expenditure, energy allocation and food and water intake of African pygmy mice. Data are for n=11 *M. mattheyi* (white) and n=11 *M. minutoides* (gray). For each box plot, the horizontal line denotes the median, the box represents the interquartile range (IQR; 25th–75th percentiles), and whiskers indicate the range of values within 1.5× IQR from the lower and upper quartiles. Outliers are indicated by filled circles and were considered in statistical analyses. (A) Minimal (EE_{min}, during the day) and maximal (EE_{max}, during the night) energy expenditure. Permutation t-tests were performed: ***P<0.001 *M. mattheyi* versus *M. minutoides*. Mean±s.d. EE of *M. mattheyi* mice was 16.4±2.5 and 35.6±4.7 mW g^{-1} during the day and night, respectively. Mean±s.d. EE of *M. minutoides* mice was 11.3±2.0 and 26.6±3.5 mW g^{-1} during the day and night, respectively. (B) Proportion of energy allocated to basal or other biological functions. Results were statistically analyzed by an ANOVA and EMMs pairwise comparisons on linear mixed models: ‡‡‡P<0.001 basal functions versus other biological functions; and *P<0.05 *M. mattheyi* versus *M. minutoides*. (C) Food and (D) water intake. Permutation t-tests were used to analyze the results: ***P<0.001 *M. mattheyi* versus *M. minutoides*.

Journal of Experimental Biology (2025) 228, jeb250373. doi:10.1242/jeb.250373

During the day, an interaction between species and type of biological function was highlighted (P=0.003), while during the night, this interaction was not significant (P=0.064). EMMs pairwise comparisons showed that, during the day, *M. mattheyi* allocated more energy to its basal functions than *M. minutoides* (P=0.039), and significantly less energy to other biological functions such as locomotion (P=0.039; Fig. 3B). Both species allocated more energy for basal functions than for other biological functions (P<0.001; Fig. 3B). During the night, the energy allocation did not differ significantly between species (P=0.20 for basal functions and P=0.20 for other biological functions; Fig. 3B). The energy allocated to basal functions was significantly higher than for other biological functions only in *M. mattheyi* (P<0.001 for *M. mattheyi* and P=0.099 for *M. minutoides*; Fig. 3B).

The respiratory quotient was similar during the active period (i.e. night-time) for both species (P=0.83): 0.92±0.04 and 0.91±0.06 for *M. mattheyi* and *M. minutoides*, respectively. At rest (i.e. during the day), the respiratory quotient was significantly lower compared with that observed during the night for both species (P<0.001). In addition, it was lower in *M. mattheyi* compared with *M. minutoides* (P=0.027): 0.70±0.06 and 0.76±0.08 for *M. mattheyi* and *M. minutoides*, respectively.

Food and water intake

Mus mattheyi ate (t=3.589, P<0.001) and drank (t=3.827, P<0.001) more than *M. minutoides* (Fig. 3C). Data concerning the frequency of food intake were firstly analyzed with ANOVA on a linear mixed model, which highlighted the interaction between species and period of the day (P=0.043). EMMs pairwise comparisons showed that both species ate and drank more regularly during the night than during the day (P<0.001 for *M. mattheyi* and P=0.001 for *M. minutoides*). *Mus mattheyi* generally ate 1±2 times in the day and 22±11 times at night, while *M. minutoides* ate on average 7±7 times in the day and 23±15 times at night. As a result, the diurnal feeding frequency in *M. mattheyi* was 6.8 times lower than that of *M. minutoides* (P=0.006).

Energy cost of movement

Statistical results highlighted that the two species covered the same distance during the day (P=0.35) and the night (P=0.24; Fig. 4A). Moreover, both species moved around much less during the day compared with the night (on average 13 times less, P<0.001; Fig. 4A). The energy cost of movement for *M. mattheyi* was 3 times higher than that for *M. minutoides* during the day (P=0.011). In contrast, during the night there was no difference between species concerning the energy used per movement (P=0.41; Fig. 4B).

Respiratory capacity of BAT and skeletal muscle

The relative proportion of BAT mass to body mass was not significantly different between the two species (t=−1.653, P=0.114): 0.66±0.20% for *M. mattheyi* and 0.83±0.27% for *M. minutoides*.

Mitochondrial oxygen consumption in BAT and skeletal muscle is reported in Table 1. The interaction between species and substrates used was significant (P=0.027) as well as the inter-individual variance (χ^2_1=98.146, P<0.001) in BAT. However, in skeletal muscle, only the inter-individual variance was significant (χ^2_1=113.480, P<0.001). In BAT, mitochondrial respiration was higher for *M. mattheyi* than for *M. minutoides* for CI-LEAK and CI-OXPHOS respiration rates (P<0.05; Table 1). With the combination of succinate (CI+CII-OXPHOS) or succinate/glycerol 3-phosphate (CI+CII+G3PDH-OXPHOS), mitochondrial BAT respiration rates

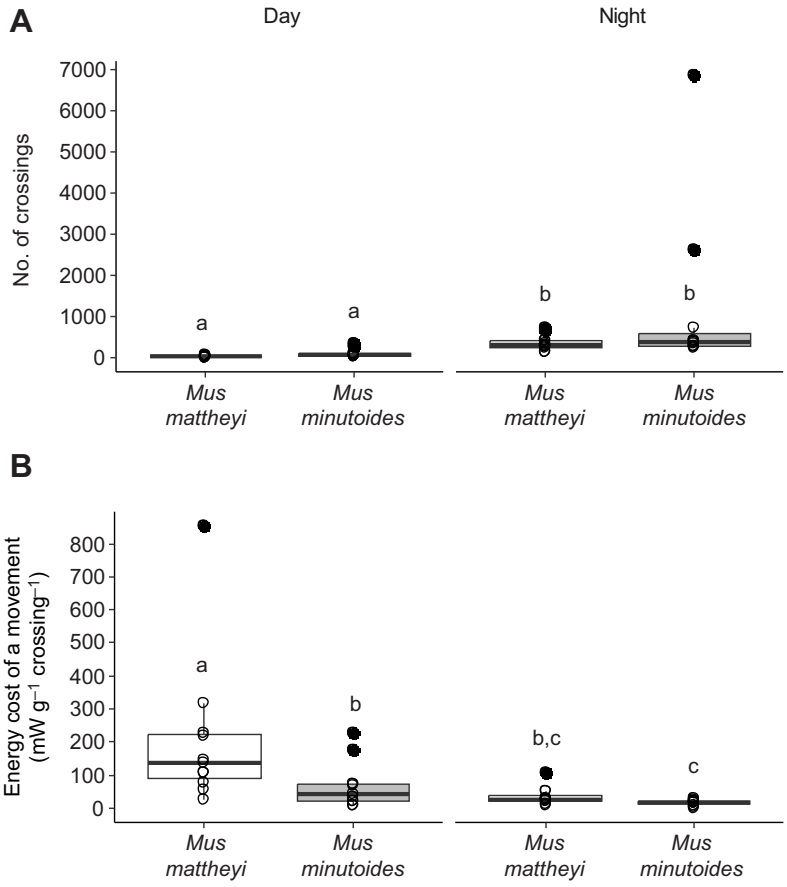

Fig. 4. Number of crossings and energy cost of movement for African pygmy mice. Data are for n=11 *M. mattheyi* (white) and n=11 *M. minutoides* (gray). For each box plot, the horizontal line denotes the median, the box represents the interquartile range (IQR; 25th–75th percentiles), and whiskers indicate the range of values within 1.5× IQR from the lower and upper quartiles. Outliers are indicated by filled circles and were considered in statistical analyses. (A) Number of crossings made by the mice. (B) Energy cost of movement calculated as the area under the curve (AUC) of total energy allocated to other functions/number of crossings for each period of time. The results were statistically analyzed by ANOVA and EMMs pairwise comparisons on the linear mixed models: different lowercase letters indicate a significant effect (P<0.05).

Journal of Experimental Biology (2025) 228, jeb250373. doi:10.1242/jeb.250373

Table 1. Mitochondrial respiration rates for different substrates in brown adipose tissue (BAT) and skeletal muscle for African pygmy mice

Mitochondrial respiration rates	*Mus mattheyi*	*Mus minutoides*
BAT		
CI-LEAK	51±16[a]	33±21[b]
CI-OXPHOS	39±13[a]	22±11[b]
CI+CII-OXPHOS	86±22[a]	60±23[a]
CI+CII+G3PDH-OXPHOS	170±56[a]	131±63[a]
MaxETS	194±71[a]	148±69[a]
Maximal capacity of COX	527±175[a]	562±300[a]
Skeletal muscle		
CI-LEAK	31±23[a]	41±16[b]
CI-OXPHOS	120±50[a]	180±63[b]
CI+CII-OXPHOS	117±47[a]	176±62[b]
CI+CII+G3PDH-OXPHOS	116±47[a]	194±93[b]
MaxETS	128±58[a]	194±96[a]
Maximal capacity of COX	192±58[a]	311±89[b]

Data are presented as means±s.d. (pmol of O_2 s^{-1} mg^{-1} tissue) for n=11 *Mus mattheyi* and n=12 *Mus minutoides*. Different lowercase letters indicate a significant effect of species (P<0.05). MaxETS, maximal capacity of the electron transfer system; COX, cytochrome *c* oxidase.

were slightly higher (+45% and +30%, respectively) in *M. mattheyi* than in *M. minutoides*, but differences failed to reach statistical significance (P=0.077 for CI-CII-OXPHOS and P=0.147 for CI-CII-G3PDH-OXPHOS; Table 1). In contrast, in the skeletal muscle, respiration of mitochondria was lower in *M. mattheyi* than in *M. minutoides* for all steady-state rates, except for MaxETS (P<0.05; Table 1).

Permutation *t*-tests were performed to study the effect of species on COX maximal capacity in BAT and skeletal muscle. COX maximal capacity was not different between species in BAT (t=−0.344, P=0.74), while in skeletal muscle it was lower in *M. mattheyi* than in *M. minutoides* (t=−3.835, P=0.004; Table 1).

The interaction between species and substrates used remained significant in BAT when mitochondrial respiration was corrected by COX maximal capacity (P=0.027), as well as the inter-individual variance (χ^2_1=37.805, P<0.001). In skeletal muscle, the inter-individual effect was significant in the model (χ^2_1=47.634, P<0.001), but no interaction was noted between species and substrates used (P=0.95). When corrected by COX maximal capacity, oxygen consumption rates of mitochondria in BAT were always higher in *M. mattheyi* than in *M. minutoides* (P<0.05; Tables S1 and S2; Fig. 5A), suggesting intrinsic mitochondrial functioning differences between the two species. In skeletal muscle, mitochondrial respiration rates expressed by COX maximal capacity were similar between the two species, with almost no effects of the different substrates used (Fig. 5B).

Enzymatic activity and relative abundance of proteins in BAT

CS activity was on average 1.3-fold higher in the BAT of *M. mattheyi* compared with that of *M. minutoides* (t=2.298, P=0.044; Fig. 6A). However, HOAD activity and CPT activity were similar between the two species (t=−1.192, P=0.24 for HOAD; t=−0.243, P=0.79 for CPT) (Fig. 6B,C). In terms of protein expression, UCP1 and ATP5b abundance in *M. mattheyi* was 2.3 and 3.5 times lower, respectively, than that in *M. minutoides* (t=−2.974, P=0.010 for UCP1; t=−2.251, P=0.049 for ATP5b). SOD2 abundance was similar between species

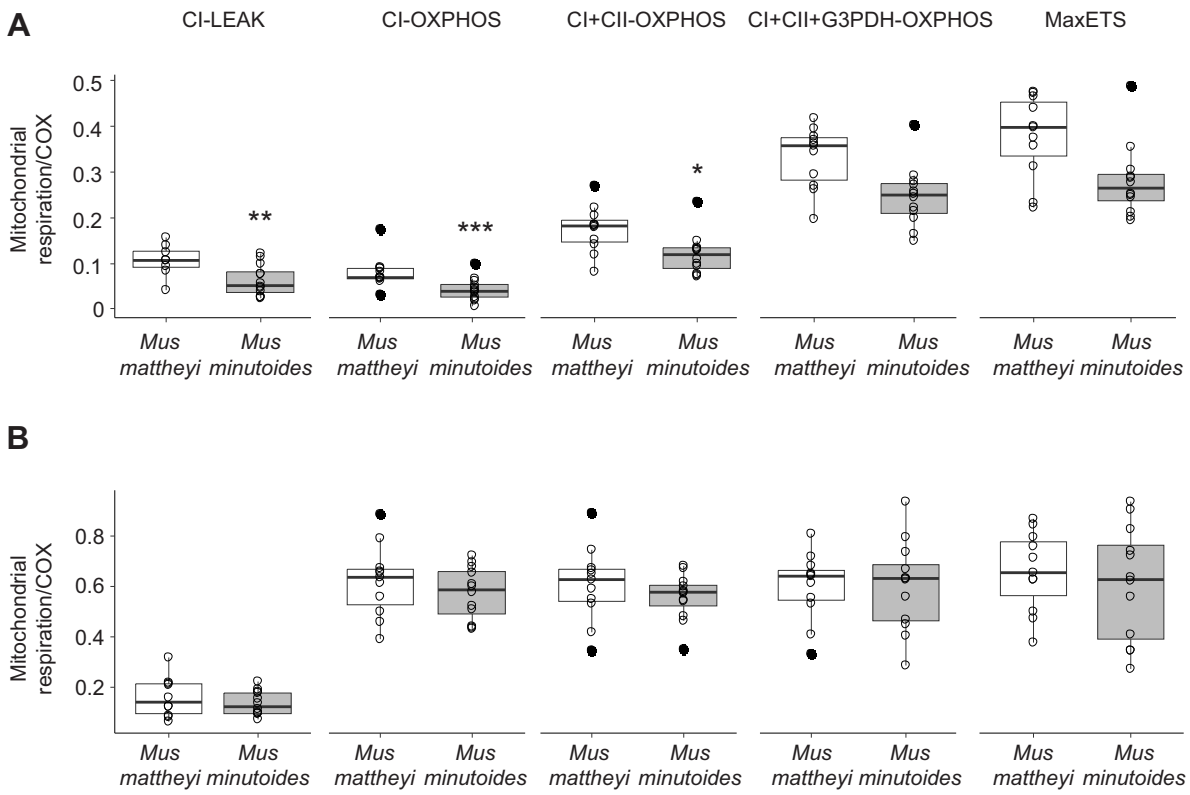

Fig. 5. Mitochondrial respiration of brown adipose tissue (BAT) and skeletal muscle from African pygmy mice. Data are for n=11 *M. mattheyi* (white) and n=12 *M. minutoides* (gray). For each box plot, the horizontal line denotes the median, the box represents the interquartile range (IQR; 25th–75th percentiles), and whiskers indicate the range of values within 1.5× IQR from the lower and upper quartiles. Outliers are indicated by filled circles and were considered in statistical analyses. (A) Mitochondrial respiration for different substrates corrected by maximal cytochrome *c* oxidase (COX) capacity in BAT. (B) Mitochondrial respiration for different substrates corrected by maximal COX capacity in skeletal muscle. The results were statistically analyzed by ANOVA and EMMs pairwise comparisons on linear mixed models: *P<0.05, **P<0.01 and ***P<0.001 *M. mattheyi* versus *M. minutoides*. MaxETS, maximal capacity of the electron transfer system.

Journal of Experimental Biology (2025) 228, jeb250373. doi:10.1242/jeb.250373

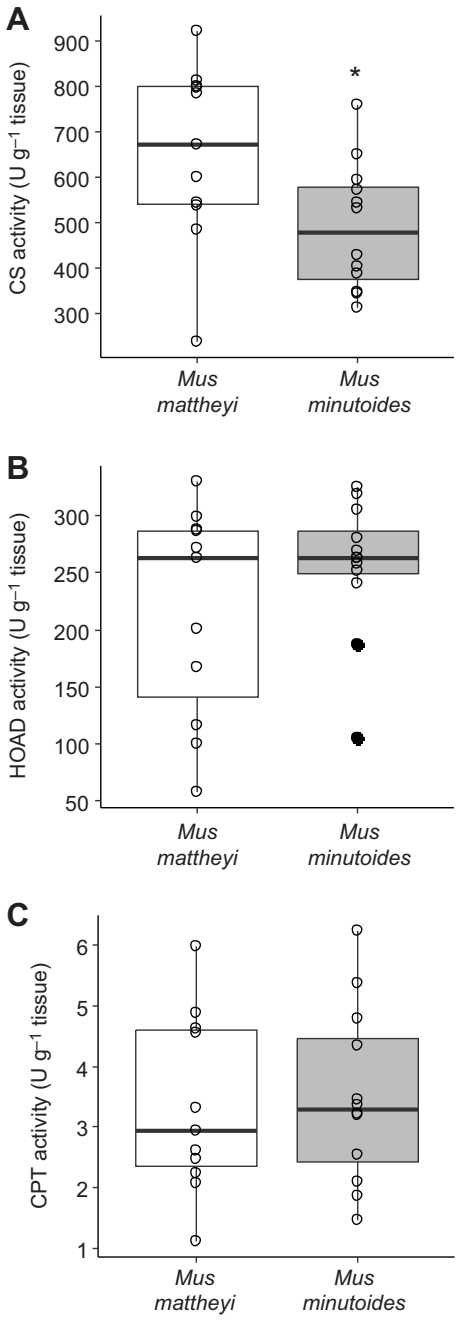

Fig. 6. Enzyme activity in BAT from African pygmy mice. Data are for *n*=11 *M. mattheyi* (white) and *n*=12 *M. minutoides* (gray). For each box plot, the horizontal line denotes the median, the box represents the interquartile range (IQR; 25th–75th percentiles), and whiskers indicate the range of values within 1.5× IQR from the lower and upper quartiles. Outliers are indicated by filled circles and were considered in statistical analyses. (A) Activity of citrate synthase (CS). (B) Activity of β-hydroxyacyl CoA dehydrogenase (HOAD). (C) Activity of carnitine palmitoyltransferase (CPT). Permutation *t*-tests were performed to statistically analyze the results: **P*<0.05 *M. mattheyi* versus *M. minutoides*.

(*t*=−0.616, *P*=0.52), whereas TOM20 was 3.2 times higher in *M. mattheyi* (*t*=3.846, *P*<0.001; Fig. 7B).

DISCUSSION

The present study aimed to investigate the possible contrasting behavioral and physiological thermogenic mechanisms in *M. minutoides* and *M. mattheyi*, the latter being the first known tiny mammalian species exhibiting reduced mitochondrial consumption together with higher efficiency for ATP production (Boël et al., 2020), leading to lower cellular heat production. Overall, the tiny *M. mattheyi* (∼6 g) expends more energy than *M. minutoides* (∼10 g) for remaining warm when exposed to an ambient temperature of 29°C, resulting in higher food consumption. By combining *in vivo* behavioral and metabolic monitoring with *in vitro* biochemical and molecular approaches, our study highlighted that, in addition to higher BAT activity, *M. mattheyi* also uses non-exercise activity to generate heat. The present data therefore underline a differential daily energy allocation in these two species of tiny mammals.

Indeed, *M. mattheyi* exhibited higher energy expenditure (EE_{min}, EE_{max} and energy expenditure over 24 h) compared with *M. minutoides*. This is consistent with publications showing a higher metabolic rate in smaller endotherms than in larger ones (Boël et al., 2020; Gavrilov et al., 2022; Glazier, 2005; Hatton et al., 2019). Body surface is positively related to body mass according to an allometric exponent <1, which leads to a greater surface area-to-volume ratio in small endotherms (Dawson and Hulbert, 1970; Reynolds, 1997; da Silva et al., 2006). As a result, small mammals have generally high energy expenditure due to greater heat loss from their body surface, which they must compensate for.

This higher mass-specific metabolic rate in *M. mattheyi* was mainly ascribed to higher non-locomotor activity (grooming and turning around, for example) compared with *M. minutoides*, and therefore was independent of the period of the day. Non-exercise activity thermogenesis (NEAT) refers to the part of daily energy expenditure resulting from spontaneous physical activity that is not specifically the result of voluntary exercise, and which will generate heat (Levine, 2002, 2004; von Loeffelholz and Birkenfeld, 2000). Hence, *M. mattheyi* may increase their non-locomotor physical activity to keep warm. This high non-exercise activity, together with a high EE_{min} and no more time resting during the day compared with *M. minutoides*, suggests that *M. mattheyi* would not use torpor as an energy-saving strategy in our experimental conditions. Consequently, compared with their size, *M. mattheyi* ate and drank more over 24 h than *M. minutoides* (Fig. 3C). In contrast, at the cellular scale, mitochondrial respiration rates in skeletal muscle were lower in *M. mattheyi* than in *M. minutoides*, as already observed in a previous study (Boël et al., 2020). The present data therefore confirm that *M. mattheyi* has less leaky (lower CI-LEAK respiration) and more efficient mitochondria compared with *M. minutoides*. The differences in mitochondrial functioning in skeletal muscle disappeared when mitochondrial respiration was normalized to maximal COX capacity (Fig. 5B). This suggests that ultimately each respiratory complex of the mitochondrial ETS contributes equally to respiration in both species.

Despite higher energy expenditure and more efficient mitochondria, which generate more ATP per oxygen molecule and nutrient consumed, *M. mattheyi* spent less time walking and running than *M. minutoides* during the day (period of inactivity). These results suggest that *M. mattheyi* does not use heat substitution through increased locomotor activity. This is consistent with the fact that *M. mattheyi* allocated more energy to its basal functions and less energy to other biological functions such as locomotion than *M. minutoides*. Although *M. mattheyi* spent less time walking/running, these mice covered the same distance as *M. minutoides* (no difference in the number of crossings). During the day, *M. mattheyi* seems to consume twice as much energy as *M. minutoides* to move around. The higher energy cost of locomotion of smaller mice is in accordance with the negative relationship that exists between the

Journal of Experimental Biology (2025) 228, jeb250373. doi:10.1242/jeb.250373

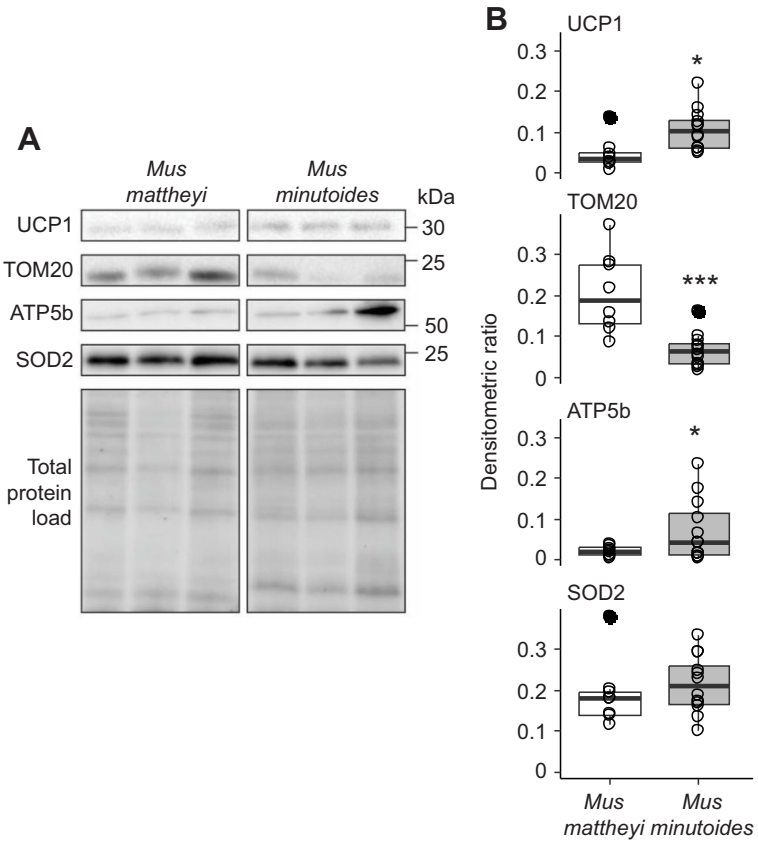

Fig. 7. Abundance of mitochondrial proteins in BAT from African pygmy mice. Data are for *n*=8 *M. mattheyi* (white) and *n*=12 *M. minutoides* (gray). (A) Representative immunoblots of three samples for uncoupling protein 1 (UCP1), mitochondrial import receptor subunit (TOM20), ATP synthase F1 subunit beta (ATP5b) levels, superoxide dismutase 2 (SOD2) and total protein load. (B) Densitometric ratio for UCP1, TOM20, ATP5b and SOD2. For each box plot, the horizontal line denotes the median, the box represents the interquartile range (IQR; 25th–75th percentiles), and whiskers indicate the range of values within 1.5× IQR from the lower and upper quartiles. Outliers are indicated by filled circles and were considered in statistical analyses. Permutation *t*-tests were used to statistically analyze the results: **P*<0.05 and ****P*<0.01 *M. mattheyi* versus *M. minutoides*.

energetic cost of running a given distance and body size in mammals: the lower the animal size, the higher the cost (Taylor et al., 1970). Part of the extra cost of locomotion may potentially arise from the higher relative body surface area of *M. mattheyi* as compared with *M. minutoides*, because of their smaller size. This would result in higher convective heat loss as the mice move around in their cage at an ambient temperature slightly below their thermoneutral zone. Such a high energy cost may also suggest a lower energetic efficiency of locomotion. This could potentially be achieved through some uncoupling of SERCA pump activity by sarcolipin and the induction of a futile cycle of calcium across sarcoplasmic reticulum membranes, which leads to the generation of heat (Bal and Periasamy, 2020; de Meis, 2002; Periasamy et al., 2017). Whether such muscle non-shivering thermogenesis is at play in *M. mattheyi* remains to be investigated; it would be consistent with the improved energetic efficiency of muscle mitochondria (Boël et al., 2020) essential to fuel the ATP-consuming processes of Ca^{2+} pumping. Another mechanism can be driven by a metabolic shift towards a preferential oxidation of fatty acid, a respiratory substrate with a lower mitochondrial efficiency (Mogensen and Sahlin, 2005; Monternier et al., 2014). Thus, the respiratory quotient of 0.7 measured during the day in *M. mattheyi* indicates that this metabolic shift would rely more on fatty acid oxidation than in *M. minutoides* (Patel et al., 2024; Prentice et al., 2013). Although modest, this metabolic shift to lipid oxidation may lead to an extra heat generation of 8–15% compared with carbohydrate-related respiratory substrate oxidation (Mogensen and Sahlin, 2005; Brand, 2005). Interestingly, all these results could provide some insight into why this species has a more restricted geographical distribution than *M. minutoides*, which is found over a wider geographical area, as far afield as South Africa. Climatic conditions in South Africa, for instance, are more contrasted, particularly in winter when food resources are scarce and night-time ambient temperatures drop below 0°C (Chikoore et al., 2024), making survival risky for such tiny nocturnal rodents.

BAT was also studied as it is known to be the tissue involved in non-shivering thermogenesis (Cannon and Nedergaard, 2004; Fenzl and Kiefer, 2014; Klingenspor, 2003). Non-shivering thermogenesis in BAT is possible thanks to the UCP1 protein, which is a mitochondrial carrier that uncouples ATP synthesis from respiration (Jones et al., 2024). In the present study, BAT UCP1 abundance was lower while TOM20 abundance was higher in *M. mattheyi* than in *M. minutoides*. As TOM20 is a protein of the outer mitochondrial membrane, a higher expression suggests that the BAT of *M. mattheyi* would contain more mitochondria than that of *M. minutoides*. Consequently, this implies that UCP1 would be less abundant in BAT mitochondria of *M. mattheyi*. This contrasts with the higher BAT mitochondrial respiration rates in *M. mattheyi* than in *M. minutoides*, irrespective of the substrate used. CS, which is the first mitochondrial enzyme involved in the tricarboxylic cycle that feeds the mitochondrial respiratory chains with NADH and $FADH_2$ (Chhimpa et al., 2023), was more active in the BAT of *M. mattheyi* than in that of *M. minutoides*. CS can also be used as a proxy for mitochondrial density (Larsen et al., 2012; Boël et al., 2023). This further indicates that the BAT of *M. mattheyi* has more mitochondria than that of *M. minutoides*. Collectively, these results suggest that BAT of *M. mattheyi* is functionally more active compared with that of *M. minutoides* because of a higher intrinsic mitochondrial functioning and higher mitochondrial density. Interestingly, we report here that the content of ATP5b, a subunit of ATP synthase involved in ATP production (Habersetzer et al., 2013), was lower in BAT from *M. mattheyi*. Combined with the

observed higher mitochondrial oxygen consumption, this could indicate a potential drop in OXPHOS coupling efficiency in this species. This hypothesis is further supported by the fact that BAT mitochondria from *M. mattheyi* exhibited a higher maximal proton leak activity than those from *M. minutoides*. It implies that the activity rather than the absolute abundance of UCP1 may be of importance in BAT thermogenesis of *M. mattheyi*. Therefore, *M. mattheyi* appears to maintain warmth, in part, by generating more heat through the dissipation of proton motive force (proton leakage) and the loose coupling of BAT mitochondria.

Conclusion

The results of the present study highlight that the two closely related study species differ in their daily energy allocation, with the tiny *M. mattheyi* investing more in basal functions and exhibiting higher non-locomotor activity as well as higher cost of movement compared with the slightly heavier *M. minutoides*. *Mus mattheyi* showed a BAT that was functionally more active and contained more mitochondria than that of *M. minutoides*. Together, these results suggest that the tiny *M. mattheyi* uses NEAT increased energy cost of movement and to a lesser extent BAT thermogenesis for remaining warm. Nevertheless, the strategies studied in this work are not exclusive; the possible use of other behavioral or physiological mechanisms, such as huddling behavior, short periods of torpor or muscle non-shivering thermogenesis cannot be excluded and remain to be investigated.

Acknowledgements

We thank Angeline Clair and Laetitia Averty (ACSED platform) for their technical assistance and for taking care of mice in the animal care facility of the Claude Bernard University.

Competing interests

The authors declare no competing or financial interests.

Author contributions

Conceptualization: M.B., D.R., Y.V.; Data curation: M.B., C.D., C.R., N.P.; Formal analysis: M.B., L.H., F.-X.D.-M., N.P.; Funding acquisition: F.V.; Investigation: M.B., L.H., C.D., C.R., F.-X.D.-M., L.T., F.V., D.R., N.P., Y.V.; Project administration: M.B., Y.V.; Resources: F.V.; Validation: M.B., D.R., N.P., Y.V.; Visualization: M.B., D.R., N.P., Y.V.; Writing – original draft: M.B., N.P.; Writing – review & editing: M.B., L.H., C.D., C.R., F.-X.D.-M., L.T., F.V., D.R., N.P., Y.V.

Funding

This work was supported by Agence Nationale de la Recherche (ANR) grant SEXREV (no. 18-CE02-0018-01). In addition, M.B. was in receipt of a Université Claude Bernard Lyon 1 fellowship (ATER).

Data and resource availability

All relevant data can be found within the article and its supplementary information.

References

Bal, N. C. and Periasamy, M. (2020). Uncoupling of sarcoendoplasmic reticulum calcium ATPase pump activity by sarcolipin as the basis for muscle non-shivering thermogenesis. *Philos. Trans. R. Soc. Lond. B Biol. Sci.* **375**, 20190135. doi:10.1098/rstb.2019.0135

Barbe, J., Watson, J., Roussel, D. and Voituron, Y. (2023). The allometry of mitochondrial efficiency is tissue dependent: a comparison between skeletal and cardiac muscles of birds. *J. Exp. Biol.* **226**, jeb246299. doi:10.1242/jeb.246299

Bates, D., Mächler, M., Bolker, B. and Walker, S. (2015). Fitting Linear Mixed-Effects Models Using lme4. *J. Stat. Softw.* **67**, 1-48. doi:10.18637/jss.v067.i01

Bergmeyer, H. U. (1983). *Methods of Enzymatic Analysis, Methods of Enzymatic Analysis: Volume II: Samples, Reagents, Assessment of Results (Bergmeyer Methods of Enzymatic Analysis)*. Wiley. https://www.abebooks.com/9783527260423/Methods-Enzymatic-Analysis-Volume-Samples-3527260420/plp (accessed 7.3.24).

Bertholet, A. M. and Kirichok, Y. (2017). UCP1: a transporter for H+ and fatty acid anions. *Biochimie* **134**, 28-34. doi:10.1016/j.biochi.2016.10.013

Bertholet, A. M. and Kirichok, Y. (2021). Mitochondrial H+ leak and thermogenesis. *Annu. Rev. Physiol.* **84**, 381. doi:10.1146/annurev-physiol-021119-034405

Boël, M., Romestaing, C., Duchamp, C., Veyrunes, F., Renaud, S., Roussel, D. and Voituron, Y. (2020). Improved mitochondrial coupling as a response to high mass-specific metabolic rate in extremely small mammals. *J. Exp. Biol.* **223**, jeb215558. doi:10.1242/jeb.215558

Boël, M., Voituron, Y. and Roussel, D. (2023). Body mass dependence of oxidative phosphorylation efficiency in liver mitochondria from mammals. *Comp. Biochem. Physiol. Part A Mol. Integr. Physiol.* **284**, 111490. doi:10.1016/j.cbpa.2023.111490

Brand, M. D. (2005). The efficiency and plasticity of mitochondrial energy transduction. *Biochem. Soc. Trans.* **33**, 897-904. doi:10.1042/BST0330897

Brand, M. D., Couture, P., Else, P. L., Withers, K. W. and Hulbert, A. J. (1991). Evolution of energy metabolism. Proton permeability of the inner membrane of liver mitochondria is greater in a mammal than in a reptile. *Biochem. J.* **275**, 81-86. doi:10.1042/bj2750081

Britton-Davidian, J., Robinson, T. J. and Veyrunes, F. (2012). Systematics and evolution of the African pygmy mice, subgenus Nannomys: a review. *Acta Oecol.* **42**, 41-49. doi:10.1016/j.actao.2012.01.001

Brown, D., Livesey, G. and Dauncey, M. J. (1991). Influence of mild cold on the components of 24 hour thermogenesis in rats. *J. Physiol.* **441**. doi:10.1113/jphysiol.1991.sp018743

Cannon, B. and Nedergaard, J. (2004). Brown adipose tissue: function and physiological significance. *Physiol. Rev.* **84**, 277-359. doi:10.1152/physrev.00015.2003

Chhimpa, N., Singh, N., Puri, N. and Kayath, H. P. (2023). The novel role of mitochondrial citrate synthase and citrate in the pathophysiology of Alzheimer's disease. *J. Alzheimers Dis.* **94**, S453-S472. doi:10.3233/JAD-220514

Chikoore, H., Mbokodo, I. L., Singo, M. V., Mohomi, T., Munyai, R. B., Havenga, H., Mahlobo, D. D., Engelbrecht, F. A., Bopape, M.-J. M. and Ndarana, T. (2024). Dynamics of an extreme low temperature event over South Africa amid a warming climate. *Weather Clim. Extrem.* **44**, 100668. doi:10.1016/j.wace.2024.100668

da Silva, J. K. L., Garcia, G. J. M. and Barbosa, L. A. (2006). Allometric scaling laws of metabolism. *Phys. Life Rev.* **3**, 229-261. doi:10.1016/j.plrev.2006.08.001

Dawson, T. J. and Hulbert, A. J. (1970). Standard metabolism, body temperature, and surface areas of Australian marsupials. *Am. J. Physiol.* **218**, 1233-1238. doi:10.1152/ajplegacy.1970.218.4.1233

de Meis, L. (2002). Ca2+-ATPases (SERCA): energy transduction and heat production in transport ATPases. *J. Membr. Biol.* **188**, 1-9. doi:10.1007/s00232-001-0171-5

Divakaruni, A. S. and Brand, M. D. (2011). The regulation and physiology of mitochondrial proton leak. *Physiology* **26**, 192-205. doi:10.1152/physiol.00046.2010

Downs, C. and Perrin, M. (1996). The thermal biology of southern Africa's smallest rodent, *Mus minutoides*. *S. Afr. J. Sci.* **92**, 282-284.

El-Gammal, Z., Nasr, M. A., Elmehrath, A. O., Salah, R. A., Saad, S. M. and El-Badri, N. (2022). Regulation of mitochondrial temperature in health and disease. *Pflugers Arch.* **474**, 1043-1051. doi:10.1007/s00424-022-02719-2

Fedorenko, A., Lishko, P. V. and Kirichok, Y. (2012). Mechanism of fatty-acid-dependent UCP1 uncoupling in brown fat mitochondria. *Cell* **151**, 400. doi:10.1016/j.cell.2012.09.010

Fenzl, A. and Kiefer, F. W. (2014). Brown adipose tissue and thermogenesis. *Horm. Mol. Biol. Clin. Investig.* **19**, 25-37. doi:10.1515/hmbci-2014-0022

Gavrilov, V. M., Golubeva, T. B., Warrack, G. and Bushuev, A. V. (2022). Metabolic scaling in birds and mammals: how taxon divergence time, phylogeny, and metabolic rate affect the relationship between scaling exponents and intercepts. *Biology* **11**, 1067. doi:10.3390/biology11071067

Girardier, L., Clark, M. G. and Seydoux, J. (1995). Thermogenesis associated with spontaneous activity: an important component of thermoregulatory needs in rats. *J. Physiol.* **488**. doi:10.1113/jphysiol.1995.sp021009

Glazier, D. S. (2005). Beyond the '3/4-power law': variation in the intra-and interspecific scaling of metabolic rate in animals. *Biol. Rev.* **80**, 611-662. doi:10.1017/S1464793105006834

Groó, Z., Szenczi, P., Bánszegi, O., Nagy, Z. and Altbäcker, V. (2018). The influence of familiarity and temperature on the huddling behavior of two mouse species with contrasting social systems. *Behav. Processes* **151**, 67-72. doi:10.1016/j.beproc.2018.03.007

Habersetzer, J., Ziani, W., Larrieu, I., Stines-Chaumeil, C., Giraud, M.-F., Brèthes, D., Dautant, A. and Paumard, P. (2013). ATP synthase oligomerization: from the enzyme models to the mitochondrial morphology. *Int. J. Biochem. Cell Biol.* **45**, 99-105. doi:10.1016/j.biocel.2012.05.017

Hammond, J. B. and Kruger, N. J. (1988). The Bradford method for protein quantitation. *Methods Mol. Biol.* **3**, 25-32. doi:10.1385/0-89603-126-8:25

Hatton, I. A., Dobson, A. P., Storch, D., Galbraith, E. D. and Loreau, M. (2019). Linking scaling laws across eukaryotes. *Proc. Natl. Acad. Sci. USA* **116**, 21616-21622. doi:10.1073/pnas.1900492116

Heldmaier, G., Braulke, L., Flick, J. and Ruf, T. (2024). Silencing of ultradian rhythms and metabolic depression during spontaneous daily torpor in Djungarian hamsters. *J. Comp. Physiol. B* **194**, 519-535. doi:10.1007/s00360-024-01573-1

Hillenius, W. J. and Ruben, J. A. (2004). The evolution of endothermy in terrestrial vertebrates: who? when? why? *Physiol. Biochem. Zool.* **77**, 1019-1042. doi:10.1086/425185
Hoole, C., Czenze, Z. J., Bennett, N. C. and McKechnie, A. E. (2019). Thermal physiology of three sympatric small mammals from southern Africa. *J. Zool.* **307**, 28-35. doi:10.1111/jzo.12613
Humphries, M. M. and Careau, V. (2011). Heat for nothing or activity for free? Evidence and implications of activity-thermoregulatory heat substitution. *Integr. Comp. Biol.* **51**, 419-431. doi:10.1093/icb/icr059
Jastroch, M., Divakaruni, A. S., Mookerjee, S., Treberg, J. R. and Brand, M. D. (2010). Mitochondrial proton and electron leaks. *Essays Biochem.* **47**, 53-67. doi:10.1042/bse0470053
Jayasundara, N., Tomanek, L., Dowd, W. W. and Somero, G. N. (2015). Proteomic analysis of cardiac response to thermal acclimation in the eurythermal goby fish *Gillichthys mirabilis*. *J. Exp. Biol.* **218**, 1359-1372. doi:10.1242/jeb.118760
Jones, S. A., Ruprecht, J. J., Crichton, P. G. and Kunji, E. R. S. (2024). Structural mechanisms of mitochondrial uncoupling protein 1 regulation in thermogenesis. *Trends Biochem. Sci.* **49**, 506-519. doi:10.1016/j.tibs.2024.03.005
Joshi, P. R. and Zierz, S. (2020). Muscle carnitine palmitoyltransferase II (CPT II) Deficiency: a conceptual approach. *Molecules* **25**, 1784. doi:10.3390/molecules25081784
Klingenspor, M. (2003). Cold-induced recruitment of brown adipose tissue thermogenesis. *Exp. Physiol.* **88**, 141-148. doi:10.1113/eph8802508
Larsen, S., Nielsen, J., Hansen, C. N., Nielsen, L. B., Wibrand, F., Stride, N., Schroder, H. D., Boushel, R., Helge, J. W., Dela, F. et al. (2012). Biomarkers of mitochondrial content in skeletal muscle of healthy young human subjects. *J. Physiol.* **590**, 3349-3360. doi:10.1113/jphysiol.2012.230185
Lasiewski, R. C., Acosta, A. L. and Bernstein, M. H. (1966). Evaporative water loss in birds - I. Characteristics of the open flow method of determination, and their relation to estimates of thermoregulatory ability. *Comp. Biochem. Physiol.* **19**, 445-457. doi:10.1016/0010-406X(66)90153-8
Levine, J. A. (2002). Non-exercise activity thermogenesis (NEAT). *Best Pract. Res. Clin. Endocrinol. Metab.* **16**, 679-702. doi:10.1053/beem.2002.0227
Levine, J. A. (2004). Nonexercise activity thermogenesis (NEAT): environment and biology. *Am. J. Physiol. Endocrinol. Metab.* **286**, E675-E685. doi:10.1152/ajpendo.00562.2003
Liwanag, H. E. M., Williams, T. M., Costa, D. P., Kanatous, S. B., Davis, R. W. and Boyd, I. L. (2009). The effects of water temperature on the energetic costs of juvenile and adult California sea lions (Zalophus californianus): the importance of skeletal muscle thermogenesis for thermal balance. *J. Exp. Biol.* **212**, 3977-3984. doi:10.1242/jeb.033282
Macherel, D., Haraux, F., Guillou, H. and Bourgeois, O. (2021). The conundrum of hot mitochondria. *Biochim. Biophys. Acta* **1862**, 148348. doi:10.1016/j.bbabio.2020.148348
Matthias, A., Ohlson, K. B. E., Fredriksson, J. M., Jacobsson, A., Nedergaard, J. and Cannon, B. (2000). Thermogenic Responses in Brown Fat Cells Are Fully UCP1-dependent: UCP2 or UCP3 do not substitute for ucp1 in adrenergically or fatty acid-induced thermogenesis. *J. Biol. Chem.* **275**, 25073-25081. doi:10.1074/jbc.M000547200
McDonald, A. E., Pichaud, N. and Darveau, C.-A. (2018). “Alternative” fuels contributing to mitochondrial electron transport: importance of non-classical pathways in the diversity of animal metabolism. *Comp. Biochem. Physiol. B Biochem. Mol. Biol.* **224**, 185-194. doi:10.1016/j.cbpb.2017.11.006
McNab, B. K. (2002). *The Physiological Ecology of Vertebrates: A View from Energetics*. Cornell University Press.
Mélanie, B., Caroline, R., Yann, V. and Damien, R. (2019). Allometry of mitochondrial efficiency is set by metabolic intensity. *Proc. R. Soc. Biol. Sci.* **286**, 20191693. doi:10.1098/rspb.2019.1693
Mogensen, M. and Sahlin, K. (2005). Mitochondrial efficiency in rat skeletal muscle: influence of respiration rate, substrate and muscle type. *Acta Physiol. Scand.* **185**, 229-236. doi:10.1111/j.1365-201X.2005.01488.x
Monternier, P.-A., Marmillot, V., Rouanet, J.-L. and Roussel, D. (2014). Mitochondrial phenotypic flexibility enhances energy savings during winter fast in king penguin chicks. *J. Exp. Biol.* **217**, 2691-2697. doi:10.1242/jeb.104505
Mota-Rojas, D., Titto, C. G., Orihuela, A., Martínez-Burnes, J., Gómez-Prado, J., Torres-Bernal, F., Flores-Padilla, K., Carvajal-de la Fuente, V. and Wang, D. (2021). Physiological and behavioral mechanisms of thermoregulation in mammals. *Animals* **11**, 1733. doi:10.3390/ani11061733
Mráček, T., Drahota, Z. and Houštěk, J. (2013). The function and the role of the mitochondrial glycerol-3-phosphate dehydrogenase in mammalian tissues. *Biochim. Biophys. Acta* **1827**, 401-410. doi:10.1016/j.bbabio.2012.11.014
Nicholls, D. G. (2006). The physiological regulation of uncoupling proteins. *Biochim. Biophys. Acta* **1757**, 459-466. doi:10.1016/j.bbabio.2006.02.005
Nowack, J. and Geiser, F. (2016). Friends with benefits: the role of huddling in mixed groups of torpid and normothermic animals. *J. Exp. Biol.* **219**, 590-596. doi:10.1242/jeb.128926
Nowack, J., Stawski, C., Geiser, F. and Levesque, D. L. (2023). Rare and opportunistic use of torpor in mammals—an echo from the past? *Integr. Comp. Biol.* **63**, 1049-1059. doi:10.1093/icb/icad067
Palma, F. R., He, C., Danes, J. M., Paviani, V., Coelho, D. R., Gantner, B. N. and Bonini, M. G. (2020). Mitochondrial superoxide dismutase: what the established, the intriguing, and the novel reveal about a key cellular redox switch. *Antioxid Redox Signal.* **32**, 701-714. doi:10.1089/ars.2019.7962
Patel, H., Kerndt, C. C. and Bhardwaj, A. (2024). Physiology, respiratory quotient. In *StatPearls* (ed. H. Patel and A. Bhardwaj). Treasure Island, FL: StatPearls Publishing.
Periasamy, M., Herrera, J. L. and Reis, F. C. G. (2017). Skeletal muscle thermogenesis and its role in whole body energy metabolism. *Diabetes Metab. J.* **41**, 327-336. doi:10.4093/dmj.2017.41.5.327
Pesta, D. and Gnaiger, E. (2012). High-resolution respirometry: OXPHOS protocols for human cells and permeabilized fibers from small biopsies of human muscle. *Methods Mol. Biol.* **810**, 25-58. doi:10.1007/978-1-61779-382-0_3
Picard, M., Taivassalo, T., Ritchie, D., Wright, K. J., Thomas, M. M., Romestaing, C. and Hepple, R. T. (2011). Mitochondrial structure and function are disrupted by standard isolation methods. *PLoS ONE* **6**, e18317. doi:10.1371/journal.pone.0018317
Pichaud, N., Ballard, J. W. O., Tanguay, R. M. and Blier, P. U. (2011). Thermal sensitivity of mitochondrial functions in permeabilized muscle fibers from two populations of *Drosophila simulans* with divergent mitotypes. *Am. J. Physiol. Regul. Integr. Comp. Physiol.* **301**, R48-R59. doi:10.1152/ajpregu.00542.2010
Prentice, R. L., Neuhouser, M. L., Tinker, L. F., Pettinger, M., Thomson, C. A., Mossavar-Rahmani, Y., Thomas, F., Qi, L. and Huang, Y. (2013). An exploratory study of respiratory quotient calibration and association with postmenopausal breast cancer. *Cancer Epidemiol. Biomarkers Prev.* **22**, 2374-2383. doi:10.1158/1055-9965.EPI-13-0511
Reynolds, P. S. (1997). Phylogenetic analysis of surface areas of mammals. *J. Mammal.* **78**, 859-868. doi:10.2307/1382944
Rolfe, D. F. and Brown, G. C. (1997). Cellular energy utilization and molecular origin of standard metabolic rate in mammals. *Physiol. Rev.* **77**, 731-758. doi:10.1152/physrev.1997.77.3.731
Schleiff, E. and Turnbull, J. L. (1998). Functional and structural properties of the mitochondrial outer membrane receptor Tom20. *Biochemistry* **37**, 13043-13051. doi:10.1021/bi9807456
Silverman, J., Suckow, M. A. and Murthy, S. (ed.) (2014). *The IACUC Handbook*, 3rd edn. Boca Raton: CRC Press. doi:10.1201/b17109
Taylor, C. R., Schmidt-Nielsen, K. and Raab, J. L. (1970). Scaling of energetic cost of running to body size in mammals. *Am. J. Physiol.* **219**, 1104-1107. doi:10.1152/ajplegacy.1970.219.4.1104
Turbill, C., Walker, M., Boardman, W., Martin, J. M., McKeown, A., Meade, J. and Welbergen, J. A. (2024). Torpor use in the wild by one of the world’s largest bats. *Proc. R. Soc. B. Biol. Sci.* **291**, 20241137. doi:10.1098/rspb.2024.1137
Veyrunes, F., Britton-Davidian, J., Robinson, T. J., Calvet, E., Denys, C. and Chevret, P. (2005). Molecular phylogeny of the African pygmy mice, subgenus *Nannomys* (Rodentia, Murinae, *Mus*): implications for chromosomal evolution. *Mol. Phylogenet. Evol.* **36**, 358-369. doi:10.1016/j.ympev.2005.02.011
von Loeffelholz, C. and Birkenfeld, A. L. (2000). Non-exercise activity thermogenesis in human energy homeostasis. In *Endotext* (ed. K. R. Feingold, B. Anawalt, M. R. Blackman, A. Boyce, G. Chrousos, E. Corpas, W. W. de Herder, K. Dhatariya, K. Dungan, J. Hofland, S. Kalra, G. Kaltsas, N. Kapoor, C. Koch, P. Kopp, M. Korbonits, C. S. Kovacs, W. Kuohung, B. Laferrère, M. Levy, E. A. McGee, R. McLachlan, M. New, J. Purnell, R. Sahay, A. S. Shah, F. Singer, M. A. Sperling, C. A. Stratakis, D. L. Trence, D. P. Wilson). South Dartmouth, MA: MDText.com, Inc.
Xu, Y., Tan, H., Liu, K., Wen, C., Pang, C., Liu, H., Xu, R., Li, Q., He, C., Nandakumar, K. S. et al. (2021). Targeted inhibition of ATP5B gene prevents bone erosion in collagen-induced arthritis by inhibiting osteoclastogenesis. *Pharmacol. Res.* **165**, 105458. doi:10.1016/j.phrs.2021.105458

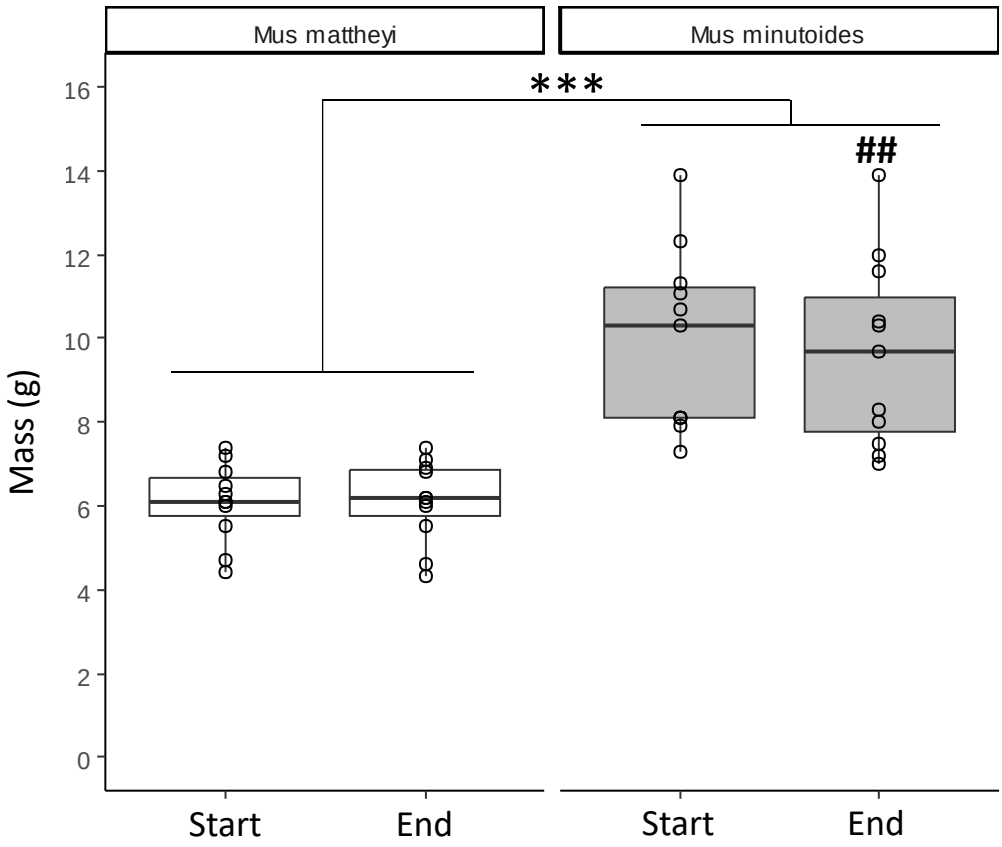

Fig. S1. Body mass variation during experiment for African pygmy mice. Body masses for *M. mattheyi* (white, n=11) and for *M. minutoides* (grey, n=11) before (Start) and after (End) behavior analysis and measurements of the energy expenditure. Results were statistically analyzed by Anova and EMMeans pairwise comparisons on a linear mixed-effect model. *** *M. mattheyi* vs *M. minutoides* ($p < 0.001$) and ## Start vs End for *M. minutoides* only ($p < 0.01$).

Table S1. Statistical results of regression models.

Other factors	Predictor	Df	X^2	p-value
Body mass				
	Species	1	29.714	<0.001
	Period (start or end of the experiment)	1	6.095	0.014
	Species x Period	1	6.447	0.011
Behavioral analysis				
Day	Species	1	0.019	0.892
	Behavior category	2	1160.609	< 0.001
	Species x Behavior category	2	13.875	< 0.001
Night	Species	1	0.005	0.944
	Behavior category	2	220.004	< 0.001
	Species x Behavior category	2	7.130	0.028
Frequency of food intake				
	Species	1	4.625	0.032
	Period	1	51.096	<0.001
	Species x Period	1	4.078	0.043

Energy allocations				
Day	Species	1	0.000	1.000
	Type of function	1	1056.416	< 0.001
	Species x Type of function	1	9.073	0.003
Night	Species	1	0.000	1.000
	Type of function	1	18.495	< 0.001
	Species x Type of function	1	3.443	0.064
Respiratory quotient				
	Species	1	2.170	0.141
	Period	1	107.478	< 0.001
	Species * Period	1	3.166	0.075
Number of crossings				
	Species	1	5.290	0.021
	Period	1	67.498	<0.001
	Species x Period	1	0.035	0.852
Energy cost of a movement				
	Species	1	8.663	0.003

	Period	1	41.705	< 0.001
	Species x Period	1	2.475	0.116
Mitochondrial respiration rates				
BAT	Species	1	5.642	0.018
	Substrate	4	687.811	<0.001
	Species x Substrate	4	10.990	0.027
Skeletal muscle	Species	1	5.510	0.019
	Substrate	4	910.019	<0.001
	Species x Substrate	4	0.763	0.943
Mitochondrial respiration rate/COX maximal capacity				
BAT	Species	1	12.413	<0.001
	Substrate	4	688.006	<0.001
	Species x Substrate	4	10.982	0.027
Skeletal muscle	Species	1	0.373	0.541
	Substrate	4	906.773	<0.001
	Species x Substrate	4	0.739	0.947

Table S2. The Estimated Marginal Means (EMMeans) difference table for pairwise comparisons of the regression results given in table S2.

Comparison	Category	Estimate	SE	df	t-ratio	p-value
Body mass						
M. mattheyi vs. *M. minutoides*	Start of the experiment	-0.200	0.036	20.2	-5.636	<0.001
	End of the experiment	-0.186	0.036	20.2	-5.232	<0.001
Start vs. end of the experiment	*M. mattheyi*	0.000	0.004	20.0	0.050	0.961
	M. minutoides	-0.014	0.004	20.0	-3.541	0.002
Behavioral analysis						
DAY *M. mattheyi* vs *M. minutoides*	Non-locomotor activity	0.318	0.107	60.0	2.966	0.004
	Locomotor activity	-0.235	0.107	60.0	-2.192	0.032
	Rest	-0.058	0.107	60.0	-0.538	0.592
NIGHT *M. mattheyi* vs *M. minutoides*	Non-locomotor activity	0.293	0.139	60.0	2.101	0.040
	Locomotor activity	-0.106	0.139	60.0	-0.758	0.451
	Rest	-0.204	0.139	60.0	-1.465	0.148
DAY Locomotor activity vs Non-locomotor activity	*Mus mattheyi*	-1.570	0.107	40.0	-14.640	<0.001
	Mus minutoides	-1.020	0.107	40.0	-9.481	<0.001
NIGHT Locomotor activity vs Non-locomotor activity	*Mus mattheyi*	-1.591	0.139	40.0	-11.424	<0.001
	Mus minutoides	-1.193	0.139	40.0	-8.564	<0.001
DAY Locomotor activity vs Rest	*Mus mattheyi*	-2.670	0.107	40.0	-24.917	<0.001
	Mus minutoides	-2.490	0.107	40.0	-23.262	<0.001

NIGHT Locomotor activity vs Rest	*Mus mattheyi*	-1.031	0.139	40.0	-7.400	<0.001
	Mus minutoides	-1.129	0.139	40.0	-8.106	<0.001
DAY Non-locomotor activity vs Rest	*Mus mattheyi*	-1.100	0.107	40.0	-10.277	<0.001
	Mus minutoides	-1.480	0.107	40.0	-13.781	<0.001
NIGHT Non-locomotor activity vs Rest	*Mus mattheyi*	0.560	0.139	40.0	4.024	<0.001
	Mus minutoides	0.064	0.139	40.0	0.458	0.891
Frequency of food intake						
M. mattheyi vs *M. minutoides*	Day	-1.798	0.614	31.6	-2.930	0.006
	Night	-0.069	0.614	31.6	-0.112	0.912
Day vs Night	*M. mattheyi*	-3.920	0.605	28.6	-6.482	< 0.001
	M. minutoides	-2.200	0.605	28.6	-3.627	0.001
Energy allocation						
DAY *M. mattheyi* vs *M. minutoides*	Basal functions	5.440	2.550	40.0	2.130	0.039
	Other functions	-5.440	2.550	40.0	-2.130	0.039
NIGHT *M. mattheyi* vs *M. minutoides*	Basal functions	4.740	3.610	40.0	1.312	0.197
	Other functions	-4.740	3.610	40.0	-1.312	0.197
DAY Basal functions vs other functions	*Mus mattheyi*	-64.100	2.550	20.0	-25.113	< 0.001
	Mus minutoides	-53.200	2.550	20.0	-20.853	< 0.001
NIGHT Basal functions vs other functions	*Mus mattheyi*	-15.730	3.610	20.0	-4.353	< 0.001
	Mus minutoides	-6.250	3.610	20.0	-1.729	0.099
Respiratory quotient						
M. mattheyi vs *M.minutoides*	Day	-0.058	0.025	40.0	-2.300	0.027
	Night	0.005	0.025	40.0	0.217	0.831

Day vs night	*M. mattheyi*	-0.217	0.025	20.0	-8.589	<0.001
	M. minutoides	-0.154	0.025	20.0	-6.072	<0.001
Number of crossing						
M. mattheyi day vs M. minutoides day		-0.698	0.418	38.3	-1.670	0.353
M. mattheyi day vs M. mattheyi night		-2.110	0.372	20.0	-5.677	< 0.001
M. mattheyi day vs M. minutoides night		-2.905	0.418	38.3	-6.956	< 0.001
M. minutoides day vs M. mattheyi night		-1.412	0.418	38.3	-3.381	0.009
M. minutoides day vs M. minutoides night		-2.208	0.372	20.0	-5.942	< 0.001
M. mattheyi night vs M. minutoides night		-0.796	0.418	38.3	-1.906	0.243
Energy cost of movement						
M. mattheyi day vs M. minutoides day		0.865	0.261	35.1	3.320	0.011
M. mattheyi day vs M. mattheyi night		1.171	0.206	20.0	5.679	< 0.001
M. mattheyi day vs M. minutoides night		1.577	0.261	35.1	6.052	< 0.001
M. minutoides day vs M. mattheyi night		0.306	0.261	35.1	1.172	0.648
M. minutoides day vs M. minutoides night		0.712	0.206	20.0	3.454	0.012
M. mattheyi night vs M. minutoides night		0.407	0.261	35.1	1.560	0.414
Mitochondrial respiration rates						
BAT *M. mattheyi* vs *M.minutoides*	CI-LEAK	0.688	0.255	34.8	2.701	0.011
	CI-OXPHOS	0.811	0.248	31.5	3.277	0.003
	CI+CII-OXPHOS	0.453	0.248	31.5	1.831	0.077
	CI+CII+G3PDH-OXPHOS	0.368	0.248	31.5	1.488	0.147
	MaxETS	0.359	0.248	31.5	1.449	0.157
	CI-LEAK	-0.439	0.196	21.0	-2.241	0.036

SKELETAL MUSCLE *M. mattheyi* vs *M.minutoides*	CI-OXPHOS	-0.413	0.195	21.0	-2.125	0.046
	CI+CII-OXPHOS	-0.412	0.195	21.0	-2.115	0.047
	CI+CII+G3PDH-OXPHOS	-0.467	0.195	21.0	-2.401	0.026
	MaxETS	-0.364	0.195	21.0	-1.872	0.075
Mitochondrial respiration rate/COX maximal capacity						
BAT *M. mattheyi* vs *M.minutoides*	CI-LEAK	0.0823	0.0284	21.0	2.902	0.009
	CI-OXPHOS	0.0810	0.0272	21.0	2.981	0.007
	CI+CII-OXPHOS	0.0731	0.0272	21.0	2.691	0.014
	CI+CII+G3PDH-OXPHOS	0.0808	0.0272	21.0	2.975	0.007
	MaxETS	0.0852	0.0272	21.0	3.136	0.005
SKELETAL MUSCLE *M. mattheyi* vs *M.minutoides*	CI-LEAK	0.0075	0.0422	21.0	0.177	0.861
	CI-OXPHOS	0.0286	0.0417	21.0	0.686	0.500
	CI+CII-OXPHOS	0.0302	0.0417	21.0	0.725	0.477
	CI+CII+G3PDH-OXPHOS	0.0027	0.0417	21.0	0.064	0.950
	MaxETS	0.0378	0.0417	21.0	0.905	0.376